Available online at www.sciencedirect.com
ScienceDirect
Continental Shelf Research 28 (2008) 159–176
CONTINENTAL SHELF RESEARCH
www.elsevier.com/locate/csr

# On the remote monitoring of *Karenia brevis* blooms of the west Florida shelf

Chuanmin Hu*, Remy Luerssen, Frank E. Muller-Karger, Kendall L. Carder, Cynthia A. Heil

*College of Marine Science, University of South Florida, 140 Seventh Ave. S., St. Petersburg, FL 33701, USA*

Received 5 May 2004; received in revised form 10 January 2007; accepted 10 April 2007
Available online 27 July 2007

**Abstract**

*In situ* surveys (1997–2002) of *Karenia brevis* distribution on the west Florida shelf were used to explain spectral remote sensing reflectance, chlorophyll-*a* concentration, and backscattering coefficient estimates derived using SeaWiFS satellite data. Two existing approaches were tested in an attempt to differentiate *K. brevis* blooms from other blooms or plumes. A chlorophyll-anomaly method used operationally by the National Oceanic and Atmospheric Administration (NOAA) sometimes correctly identified *K. brevis* blooms but also generated false positives and false negatives. The method identified approximately 1000 $km^2$ of high chlorophyll-anomalies ($>1\,mg\,m^{-3}$) off southwest Florida between the 10 and 50-m isobaths nearly every day from summer to late fall. Whether these patches were *K. brevis* blooms or not is unknown. A second method used a backscattering:chlorophyll-*a* ratio to identify *K. brevis* patches. This method separated *K. brevis* from other blooms using *in situ* optical data, but it yielded less satisfactory results with SeaWiFS data. Spectral reflectance ($R_{rs}$) estimates for *K. brevis* blooms, diatom blooms, and coastal river plumes are statistically similar for many cases. Large pixel size, shallow water, and imperfect algorithms distort satellite retrievals of bio-optical parameters in patchy blooms. At present, a combination of chlorophyll-*a*, chlorophyll-anomaly, backscattering:chlorophyll-*a* ratio, RGB composites, MODIS fluorescence data, as well as time-series analysis and ancillary data such as winds, currents, and sea surface temperature can improve *K. brevis* bloom assessments. Progress in atmospheric correction and bio-optical inversion algorithms is required to help improve capabilities to monitor *K. brevis* blooms from space. Further, satellite sensors with improved radiometric capabilities and temporal/spatial resolutions are also required.


*Keywords:* Harmful Algal Bloom; Ocean color; Remote sensing; Chlorophyll; Backscattering; Fluorescence

## 1. Introduction

The west Florida shelf (WFS) has great national environmental significance because of its natural resources and beauty. This is a sensitive environment located in close proximity to growing urban, industrial, and agricultural stressors. Over history, this region also has experienced frequent blooms of the toxic dinoflagellate *Karenia brevis* (*K. brevis*, also previously called *Gymnodinium breve*). *K. brevis* blooms have an impact on local fauna and carry significant human health risks (Anderson, 1995). The organism produces brevetoxins, which can

*Corresponding author. Tel.: +1 727 5533987.
*E-mail address:* hu@marine.usf.edu (C. Hu).

0278-4343/$ - see front matter © 2007 Elsevier Ltd. All rights reserved.
doi:10.1016/j.csr.2007.04.014

accumulate in shellfish (e.g., oysters and clams) and cause mortalities of fish, reptiles, birds and marine mammals. The toxins can be airborne in aerosols and cause eye and respiratory system irritation in humans. For this reason, these blooms fall under the broad category of harmful algal blooms (HABs). Traditionally they are also referred to as "red tides", but they can make waters of the WFS appear brown, red, or even black. In this text, the terms *K. brevis* blooms and red tides are used interchangeably.

Red tides have been reported practically every year on the WFS. The frequency, duration, and distribution appear to have increased in recent years (Morton and Burklew, 1969; Williams and Ingle, 1972; Steidinger and Ingle, 1972; Steidinger and Joyce, 1973; Steidinger and Haddad, 1981; Anderson, 1995; Steidinger et al., 1998; Walsh and Steidinger, 2001; Brand and Compton, 2007). However, it is unclear if this tendency is real or apparent, due to increased sampling efforts. This trend has been the subject of substantial discussion within the scientific community.

The exact mechanisms of initiation, maintenance and demise of red tides are still unknown. Several hypotheses have been proposed (e.g., Walsh and Steidinger, 2001; Walsh et al., 2006; Hu et al., 2006) but remain to be tested. Historical data suggest that red tides are initiated offshore in nutrient-poor waters (Tester and Steidinger, 1997), and that they move toward shore by winds and currents either at the surface or in shoreward subsurface currents, where they concentrate near fronts or intensify utilizing new nutrients from coastal runoff (Walsh et al., 2006).

Timely observation of *K. brevis* blooms is essential in all aspects of red tide studies, including hypothesis testing, environmental assessment, ecological modeling, and prediction and mitigation. Significant efforts have been invested in HAB monitoring (e.g., NOAA's Monitoring and Event Response for Harmful Algal Blooms or MERHAB program), most of which relied on field measurements since this is currently the only accurate means to differentiate *K. brevis* from various other phytoplankton species. However, field surveys have limited spatial coverage and temporal frequency. This lack of synopticity has made it difficult to understand the geographic origin, extent and dispersal of WFS red tides.

Remote sensing of the color of the ocean is effective for monitoring water quality, including phytoplankton blooms and river plumes (e.g., SWFDOG, 2002; Hu et al., 2003a). Of particular interest are ocean color data collected from satellite platforms like the Sea-viewing Wide Field-of-view Sensor (SeaWiFS, McClain et al., 1998) and the Moderate Resolution Imaging Spectroradiometer (MODIS, Esaias et al., 1998). These offer synoptic coverage, frequent revisits, and high sensitivity. However, the question remains whether satellite imagery can be used to discriminate red tides from other blooms (e.g., diatom blooms) or land runoff plumes. Our objectives with this study were to review the remote sensing technology available to evaluate red tide phenomena and to assess two existing approaches. We conclude with a brief discussion on future directions for remote monitoring of HABs.

## 2. Background: remote detection of red tides

Detection of red tides via remote sensing is a highly desirable goal. Current ocean color sensors provide near-daily operational and synoptic monitoring of the coastal ocean, and occasionally multiple observations per day are possible by combining data from SeaWiFS and MODIS (Terra for morning pass and Aqua for afternoon pass). The next operational series of polar-orbiting weather satellites, the National Polar-Orbiting Operational Environmental Satellite System (NPOESS) and the NPOESS Preparatory Mission (NPP), will carry the Visible/Infrared Imager/Radiometer Suite (VIIRS) of instruments, which will provide ocean color measurements. It is therefore useful to explore the capabilities of this class of sensors and understand the potential to differentiate red tides from other blooms or river plumes in coastal areas.

Optical means have been used to differentiate between various phytoplankton groups for some time. For example, white coccolithophores and *Trichodesmium* spp. are distinct in their backscattering characteristics (Balch et al., 1991; Subramaniam et al., 1999). Discrimination between *K. brevis* and other groups using optical signals is difficult (Schofield et al., 1999; Millie et al., 1997; Cullen et al., 1997; Lohrenz et al., 1999; Kirkpatrick et al., 2000) and results have not been conclusive. Absorption spectra of cultured *K. brevis* show some distinctive characteristics in the fourth derivative at some wavelengths (Millie et al., 1997), but application of such lab techniques in the field may be problematic because of the limited sensitivity of field

instruments and interference from other water constituents (e.g., detritus or dissolved materials).

The color of the ocean, and specifically the spectral water-leaving radiance ($L_w(\lambda)$), is determined by the various inherent optical properties (IOPs) such as total absorption ($a$) and backscattering ($b_b$) coefficients, as well as by the illumination condition (downwelling solar irradiance, $E_d(\lambda)$). IOPs are further determined by various optically active constituents (OACs) including phytoplankton, detritus, colored dissolved organic matter (CDOM), suspended sediments, and water molecules. The concentrations of the OACs vary in both space and time, and this affects remote sensing reflectance spectra [$R_{rs}(\lambda) \equiv L_w(\lambda)/E_d(\lambda)$] (Fig. 1).

*K. brevis* cells contain highly absorbing pigmentation (chlorophyll-*a* and accessory pigments) and in principle may be differentiated from other cells by their color. Chlorophyll-*a* content ranges from approximately ~8.5 pg cell$^{-1}$ for natural populations to ~25 pg/cell for cultured populations (Evens et al., 2001). Assuming 10 pg cell$^{-1}$, a concentration

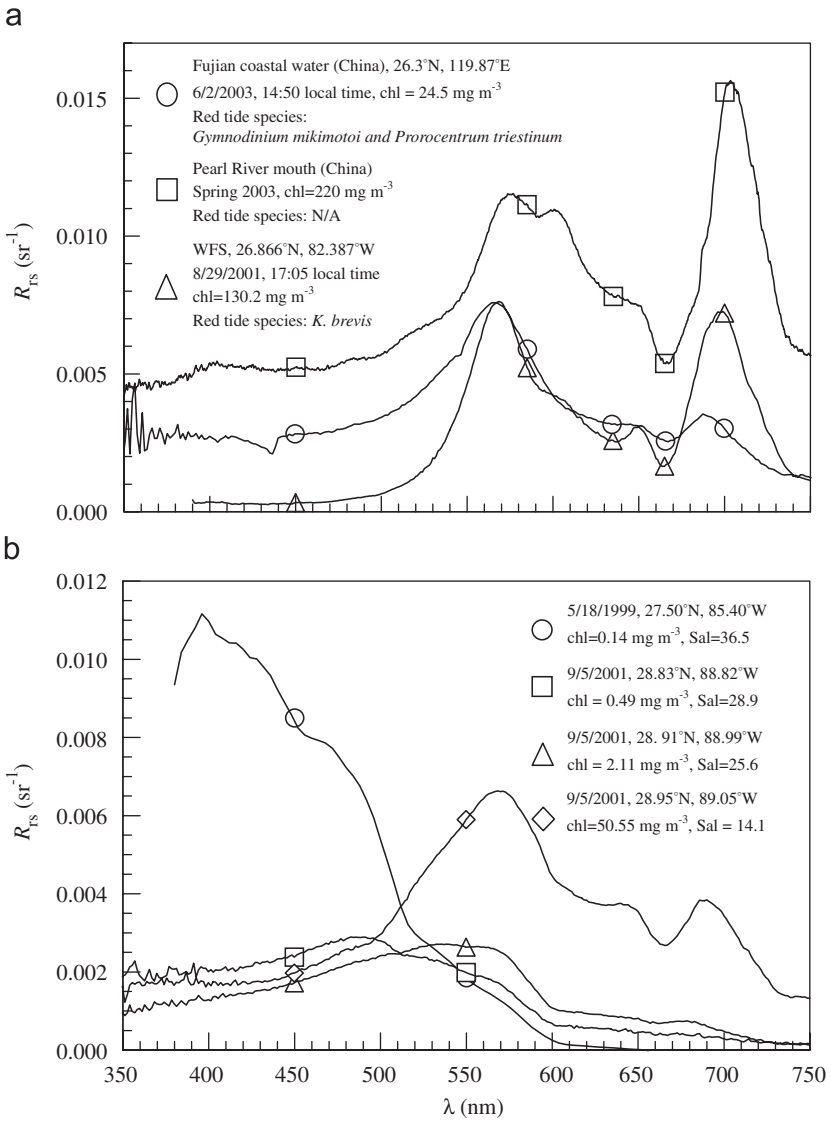


Fig. 1. Remote sensing reflectance spectra obtained from (a) several red tide blooms in Chinese coastal waters and on the west Florida shelf (WFS) and (b) clear water in the Gulf of Mexico and non-red tide blooms near the Mississippi River mouth. Red tide data courtesy of Xiaoxin Ma (Xiamen University, China), Chuqun Chen (South China Sea Institute of Oceanography), and Jennifer Cannizzaro (University of South Florida), respectively.

of $10^4$ cells $L^{-1}$ implies 0.1 mg $m^{-3}$ of chlorophyll-*a*. Cell concentrations of $5 \times 10^4$–$10^5$ cell $L^{-1}$ may cause fish kills (Steidinger et al., 1998). However, 0.1 mg $m^{-3}$ of chlorophyll-*a* is close to the background levels in the open Gulf of Mexico. To be detectable by a satellite remote sensor, cell concentrations need to be several times larger, typically in the range of $10^5$ or higher. When *K. brevis* concentration is about $10^6$ cells $L^{-1}$, chlorophyll-*a* may be as high as 10 mg $m^{-3}$ and the color is noticeably dark red, brown or possibly black.

Fig. 1a shows typical $R_{rs}$ spectra from red tides on the WSF and from toxic blooms of other regions, and Fig. 1b shows the color of open Gulf of Mexico waters and river plumes. The spectra of the blooms in Chinese and WFS coastal waters are different in the shorter wavelengths, due possibly to the high sediment content in the former region. However, the spectral shapes are similar and both differ substantially from other water types (Fig. 1b). Similar results were found by Cannizzaro et al. (this issue).

In practice, satellite remote sensing data suffer from cloud cover, errors in the radiometric calibration, and uncertainty in atmospheric correction and bio-optical inversion algorithms. Kahru and Mitchell (2001) studied non-toxic red tides and other phytoplankton blooms off California, and found that those particular red tides had peculiar ultraviolet signatures. These wavelengths, unfortunately, are not available in current ocean color sensors. Zhang et al. (2000) used computer intelligence and spectral analysis of coastal zone color scanner (CZCS) imagery to detect red tides on the WFS. Similarly, Zhang (2002) used a neural classifier to identify extensive red tide patches that occurred on the WFS in 2001 based on spectral information collected with the SeaWiFS. However, the same approach using data from other years did not yield convincing results. Stumpf (2001) and Stumpf et al. (2003a) proposed to use chlorophyll-*a* anomaly (hereafter referred to as chlorophyll-anomaly) as an index for possible red tide occurrence. This method and other ancillary data (wind, historical data) are being used by NOAA's CoastWatch program for HABs observation. Recently, Cannizzaro et al. (this issue) used a large *in situ* dataset (EcoHAB and HyCODE cruises) and a bio-optical model (Carder et al., 1999) to show a distinct signature in the $b_b$:chlorophyll-*a* ratio for red-tides compared with other blooms.

We test these approaches here using extensive satellite and *in situ* data to help determine their utility as monitoring tools. We conclude the manuscript with a brief discussion of future requirements in research and technology to improve our ability to study and monitor coastal and shelf waters from space.

## 3. Data and methods

### 3.1. Satellite data

Ocean color data for 1997–2002 were obtained from SeaWiFS with the processing algorithms embedded in NASA's software package "SeaDAS4.4". An iterative approach (Arnone et al., 1998; Stumpf et al., 2003b) based on the Gordon and Wang (1994) algorithm was used to correct for atmospheric interference to obtain spectral $R_{rs}$ data. These were used in the OC4 (O'Reilly et al., 2000) and semi-analytical (Carder et al., 1999, global parameterization) algorithms to estimate chlorophyll-*a* concentrations. The $R_{rs}$ data were also used in a spectra-matching algorithm (Lee et al., 1999; Hu et al., 2003b) to estimate total absorption and backscattering coefficients. The satellite data were downlinked, processed, and archived in near real-time at the University of South Florida.

Ocean color data from MODIS were processed with software from the University of Miami (RSMAS) to generate $R_{rs}$, chlorophyll-*a* concentration, CDOM absorption, and fluorescence line height (FLH) products. Due to uncertainties in MODIS/Terra sensor calibration, only FLH data from MODIS/Aqua were used to verify whether a dark feature was caused by a phytoplankton bloom or some other phenomenon like a river plume (Hu et al., 2005).

### 3.2. In situ data

*K. brevis* cell counts for the period 1997–2002 were obtained from the Florida Fish and Wildlife Research Institute (FWRI) Harmful Algal Bloom Historical Database. Fig. 2a shows the location and frequency of the *in situ* sampling from late 1997 to early 2002. Samples were collected by FMRI employees, local agencies, volunteers, and University of South Florida researchers along the Florida coast with no standardized collection procedure. Some samples were counted live, and some were preserved in Lugols iodine solution for later counting. Some counts were made using the Utermohl method with an inverted microscope

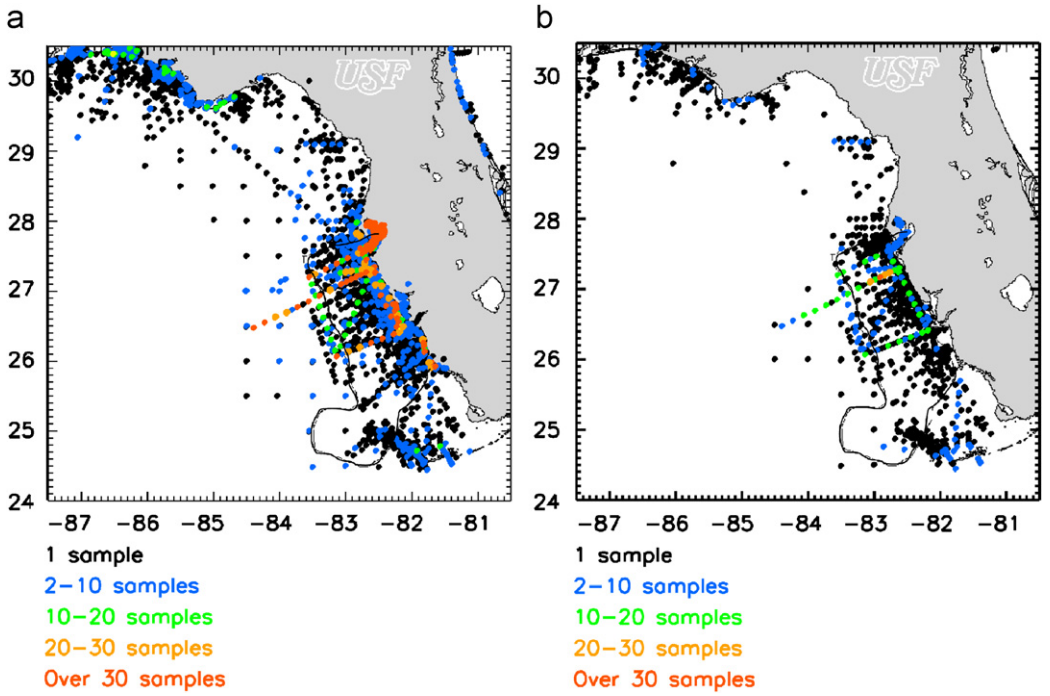


Fig. 2. Location and frequency of *K. brevis* sampling from late 1997 and early 2002 (data courtesy of FMRI). (a): All samples; (b): samples only when SeaWiFS matching pairs (i.e., at the same location and on the same day) is found.

and some with a standard microscope. Occasionally (but not routinely) some other data, such as chlorophyll-*a* concentration and hydrographic data, were collected at the sampling site. Date was recorded for every sample, but time was missing from many entries. Due to variations in counting technique, all count data were reported in increments of 333 cells $L^{-1}$ (i.e., 333 cells $L^{-1}$ was the minimum detectable level of the technique).

For satellite and *in situ* matchups, typically only satellite observations within 3 h of *in situ* data collections should be used (e.g., NASA's SeaBASS database; Bailey et al., 2000). Since there was no time information available for the *in situ* red tide data, a matching SeaWiFS data point (either $R_{rs}$, chlorophyll, or $b_b$) was sought for the sample location within the same day and tabulated if not obscured by cloud cover. To reduce errors from digitization noise, a median value from a $3 \times 3$ box was used (Hu et al., 2001). The bottom can contribute to water-leaving radiance in clear waters (Lee et al., 1999). Cannizzaro et al. (this issue) considered only waters with chlorophyll-*a* concentrations greater than about 1.5 mg $m^{-3}$ as candidate waters for discriminating red tides. At these concentrations, the blooms obscure the bottom where the depth is greater than about 15 m. Further variability in the comparisons is expected because of a mismatch in the scales observed, with SeaWiFS data covering approximately 1 $km^2$ per pixel (and a $3 \times 3$ pixel box was sampled), while each paired *in situ* observation effectively represents the size of a small bottle (a few hundred milliliters).

As a compromise to ensure a sufficient number of *in situ* data points for a robust analysis, and to reduce some bottom effects, we restricted our study to shelf waters where the bottom was 10–50 m depth (Fig. 2). This spans an area from approximately 12–90 km offshore. We examined the region extending from Tampa Bay to the Florida Keys, and further excluded near-shore areas that had apparent influence of local river runoff plumes. Distribution and frequency of the matching *in situ*-satellite data pairs are also shown in Fig. 2b.

### 3.3. Test of the NOAA chlorophyll–anomaly method

The chlorophyll-*a* anomaly, used operationally by NOAA to issue HAB alerts for the west Florida shelf was estimated as the difference between the current data and a 2-month historical average computed 2 weeks earlier (Stumpf et al., 2003a).

An anomaly threshold of $1\,mg\,m^{-3}$ was used to detect new blooms, which were catalogued as likely to be red tides during late summer and fall and for waters on the WFS away from river mouths (Stumpf et al., 2003a). The area coverage (in $km^2$) of the anomalies ($>1\,mg\,m^{-3}$) for waters within the region of interest (i.e. between the 10-m and 50-m isobaths) is summarized in Fig. 4. We used all daily imagery where cloud cover was less than 50% over this subregion.

The *K. brevis* cell counts were compared with the matching satellite-derived chlorophyll–anomaly data, and six cases were defined to test the robustness of the method in identifying red tides:

*Case* 1: Anomaly $>1\,mg\,m^{-3}$ and cell counts $>10^5\,L^{-1}$.

*Case* 2: Anomaly $>1\,mg\,m^{-3}$ and cell counts $<10^5\,L^{-1}$ but $>0\,L^{-1}$.

*Case* 3: Anomaly $>1\,mg\,m^{-3}$ and cell counts $=0\,L^{-1}$.

*Case* 4: Anomaly $<1\,mg\,m^{-3}$ and cell counts $<10^5\,L^{-1}$ but $>0\,L^{-1}$.

*Case* 5: Anomaly $<1\,mg\,m^{-3}$ and cell counts $>10^5\,L^{-1}$.

*Case* 6: Anomaly $<1\,mg\,m^{-3}$ and cell counts $=0\,L^{-1}$.

Note that due to the instrument limit, 0 counts actually meant below instrument detection limit. The case of "anomaly $<1\,mg\,m^{-3}$" included negative anomalies but excluded cloud cover.

### 3.4. Test of the $b_b$:chlorophyll-*a* ratio method

We divided the *in situ* dataset into four groups: $<10^3$ cells $L^{-1}$, between $10^3$ and $10^4$ cells $L^{-1}$, between $10^4$ and $10^5$ cells $L^{-1}$, and $>10^5$ cells $L^{-1}$ (Cannizzaro et al., this issue). For each group we then plotted particulate backscattering coefficient at 555 nm ($b_{bp}555$; Lee et al., 1999; Hu et al., 2003b) against chlorophyll-*a* (Carder et al., 1999; O'Reilly et al., 2000), and studied the data for possible correlations.

### 3.5. Spectral analysis

Both phytoplankton blooms and river plumes generally appear dark in ocean color satellite imagery because both phytoplankton and CDOM absorb blue and blue-green light. Viewed by an *in situ* observer, these features may appear to have different colors. For example, phytoplankton blooms can have a blue-green or green color, but *K. brevis* blooms appear brownish or reddish. River plumes and other coastal runoff can be brown, yellow, or even red. We measured the spectral remote sensing reflectance ($R_{rs}$) properties of various features on the west Florida shelf with the intent of assessing whether we could use satellite data to differentiate them by their color. A standard *t*-mean test (unpaired) was run on each of the spectra (6 wavelengths) for low chlorophyll-*a* ($1–2\,mg\,m^{-3}$) and mid-chlorophyll-*a* ($2–5\,mg\,m^{-3}$) levels, respectively.

## 4. Results

### 4.1. Chlorophyll–anomaly

The SeaWiFS chlorophyll-*a* anomaly images for 18 January and 17 October 2000 (Figs. 3a and b, respectively) were effectively identical to those shown in Stumpf et al. (2003a). This suggests that our data processing methods were consistent with those used by NOAA. The high anomaly patches ($>1\,mg\,m^{-3}$) in the elliptical zones outlined in Fig. 3 contained high *K. brevis* cell counts, according to *in situ* water sample analysis (data not shown). For these dates, the NOAA chlorophyll–anomaly method was successful in identifying red tides.

A more thorough examination of all images available between 1998 and 2003 indicated that there were high chlorophyll–anomaly patches nearly every day. Waters near river mouths or in very shallow ($<10\,m$) areas were purposefully excluded from the analysis since the SeaWiFS satellite data are subject to larger uncertainties in these regions due primarily to imperfect algorithms. However, even within our restricted area of interest (white outline in Fig. 3) and using only imagery with $<50\%$ cloud cover within this limited subregion (which reduced the number of daily images to about 100–130 per year), high anomaly patches were found nearly every day when an image was available (Fig. 4).

To minimize false red tide positives during the course of a year, Stumpf et al. (2003a) recommended use of the NOAA chlorophyll–anomaly method only for late summer to fall periods, when red tides have been more frequent over history. Still, this method identified $\sim1000\,km^2$ anomaly areas between the 10 and 50-m isobaths nearly every day over this time period. Also, there was little interannual variability in the size of high anomaly areas for the period 1998–2003. The anomaly method

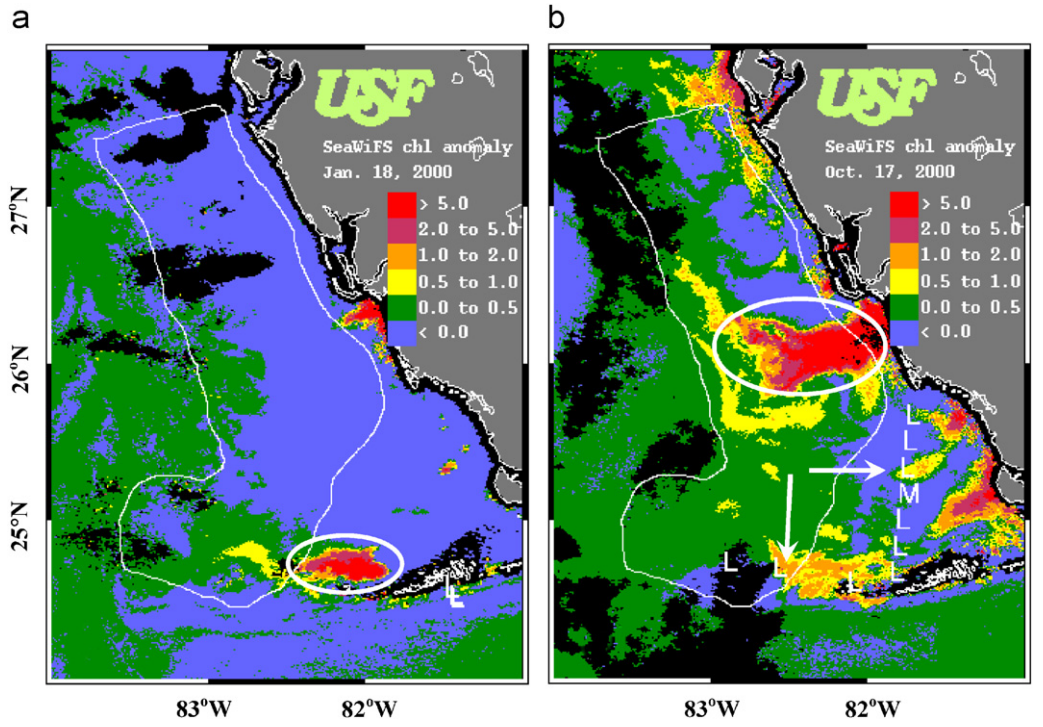


Fig. 3. Chlorophyll–anomaly imagery from SeaWiFS (OC4 algorithm) on 18 January and 17 October 2000, respectively. The anomaly is defined as the difference between the current (daily) value and a 2-month average 2 weeks ago. The high anomaly patches ($>1\,mg\,m^{-3}$) in the elliptical outlines were found with high *K. brevis* cell counts from *in situ* water sample analysis. The white irregular outlines delineate area of interest where statistics is performed (Fig. 4), namely from 10 to 50 m water depth from Tampa Bay to the Florida Keys. "H," "M," and "L" means high ($>10^5\,L^{-1}$), medium ($<10^5\,L^{-1}$ but $>10^3\,L^{-1}$), and low ($<10^3\,L^{-1}$) *K. brevis* counts concentration, respectively, for the same day.

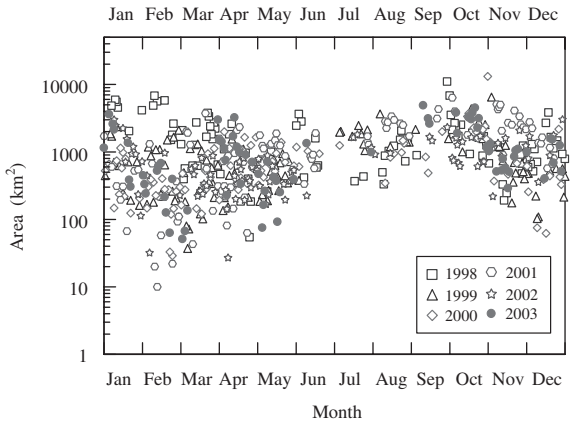


Fig. 4. Daily surface area coverage of high chlorophyll–anomaly ($>1\,mg\,m^{-3}$) within the subregion outlined in Fig. 3 from 1998 to 2003. Only imagery with <50% cloud cover over this subregion were used. Note that the anomaly approach has been used by NOAA for summer and fall only.

suggests extensive, persistent offshore blooms every year, but there were no widespread reports of red tides by local fishermen during these years.

Unfortunately, for most of the patches identified as possible red tides by the anomaly method there are no *in situ* observations to validate the assessments. Yet, available matching pairs for the SW Florida coastal waters between 10 and 50 m isobaths (region outlined in Figs. 2 and 3) for 1997–2002 were grouped into the six cases mentioned above (Fig. 5). For the periods July–December, the occurances of the six cases were $1.9\pm2.7\%$, $2.7\pm1.3\%$, $4.1\pm1.7\%$, $17.8\pm4.8\%$, $4.6\pm6.2\%$, and $68.8\pm14.8\%$, respectively. For the entire years the statistics were similar.

This small number of positive matches is mainly due to the fact that most data were from non-bloom waters (e.g., $68.8\pm14.8\%$), but also partially due to the limited size of our region of interest and 1-day concurrency restriction for match-ups. The percentage increases if these limits are relaxed. The largest number is Case 6: no anomaly and no bloom, because most of the sampled waters in between the 10–50 m isobaths should contain no *K. brevis*. If this category were exludued in measuring the success

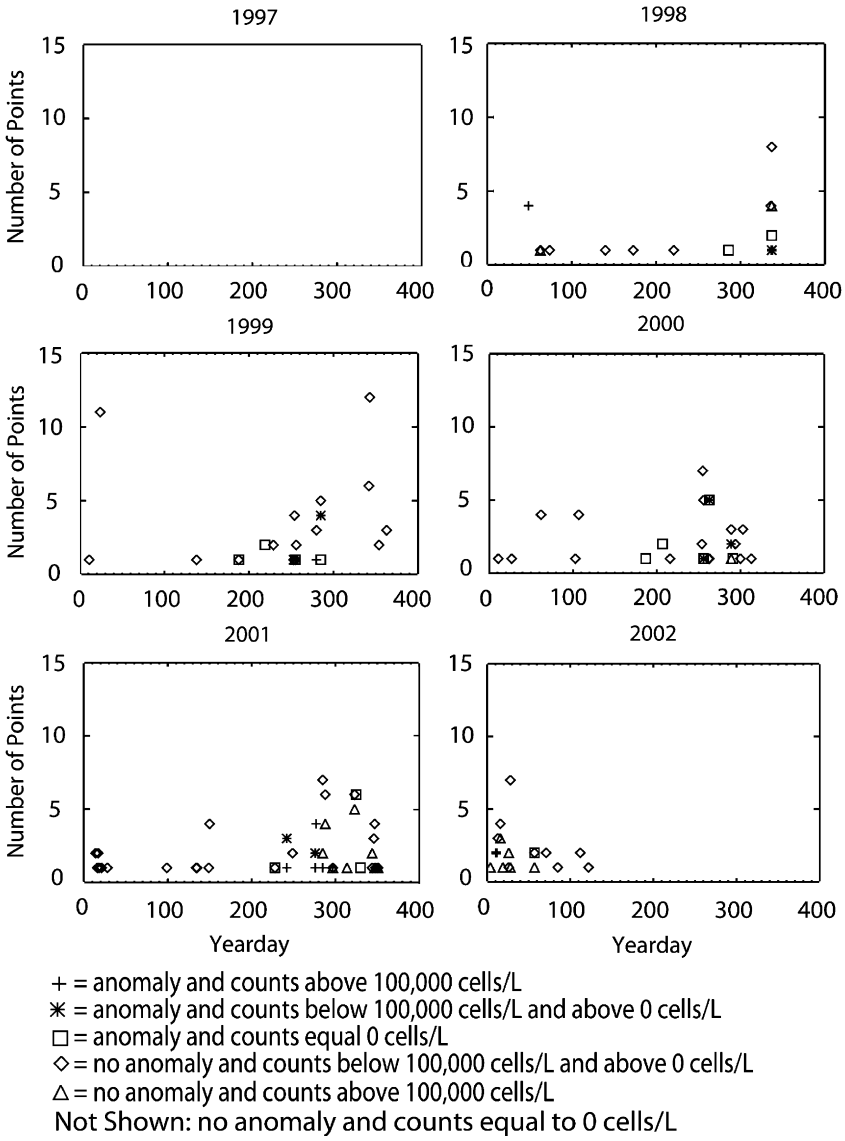


Fig. 5. Statistics of the six cases for all matching pairs of *in situ* cell counts and SeaWiFS chlorophyll–anomaly data within the area of interest (outlined in Fig. 3) from late 1997 to early 2002 (Fig. 2b). From July to December, average occurrences of the six cases were: $1.9\pm2.7\%$, $2.7\pm1.3\%$, $4.1\pm1.7\%$, $17.8\pm4.8\%$, $4.6\pm6.2\%$, and $68.8\pm14.8\%$, respectively. Note that for clarity the symbols for Case 6 were not overlaid in the figure. Note that due to the instrument limit, 0 counts actually meant below detection limit. "No anomaly" meant that anomaly was $<1\,\mathrm{mg\,m^{-3}}$, including negative anomalies but excluding cloud cover.

rate of the method, 63% of the matching pairs (Cases 1 and 4) would be regarded as successful, while the ramaining 37% (Cases 2, 3, 5) would yield either false positives or false negatives. Note that because of the cloud cover and unevenly distributed *in situ* sampling (in both spatial and temporal domains) and in particular, because of the coherency of red tides in either space or time (i.e., multiple matchups may actually be due to one single red tide event), such numbers may only be treated in a relative sense.

Fig. 6 shows *K. brevis* counts versus SeaWiFS chlorophyll-*a* concentration (OC4 algorithm). There was generally a positive correlation between the OC4 chlorophyll-*a* and *K. brevis* concentration (except for zero *K. brevis* counts). However, because of the way the NOAA method computes anomalies, a prolonged bloom may result in a low anomaly

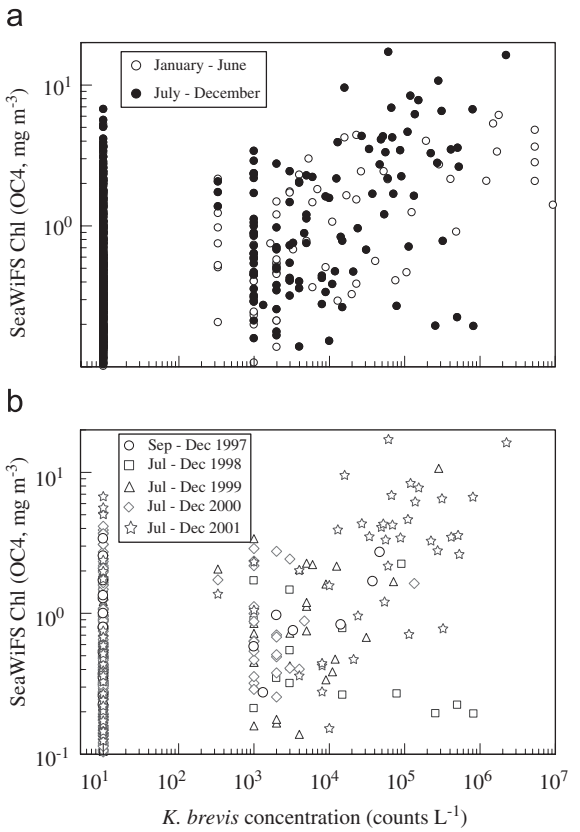


Fig. 6. Comparison of SeaWiFS-derived chlorophyll concentration (OC4 algorithm) and *K. brevis* concentration from *in situ* sampling for the area outlined in Fig. 3. (a) Data were divided into two groups: January–June and July–December and (b) individual years are shown for July–December. All data of 0 counts are shown as having a minimal value of 10.

(e.g., Fig. 7c) or even no chlorophyll–anomaly. Examining a combination of chlorophyll-*a* and chlorophyll–anomaly images helped reduce this problem in cases of extended bloom periods.

There are also some false positives (high chlorophyll–anomaly but no *K. brevis* bloom) and false negatives (*K. brevis* bloom but no high chlorophyll–anomaly). Fig. 7 shows some examples of false positives (a and b) and false negatives (c and d), as determined by concurrent *K. brevis* count data. On 21 November 2001, a high-anomaly patch (Fig. 7b) had low *K. brevis* counts. The patch was in the same area as a bloom identified in September 2001 as having high *K. brevis* counts. On 7 July 1999 (Fig. 7a) and 17 October 2000 (Fig. 3b) other false positives were obtained, with similar false positives several days before and after each of these dates. While one high-anomaly patch (outlined in the circle in Fig. 3b) was found to have high *K. brevis* concentrations, several other high-anomaly patches, including waters near the Florida Keys, showed low *K. brevis* concentrations.

Several false negatives occurred during known *K. brevis* blooms, for example 3 December 1998 (Fig. 7). The causes of such false negative events was unclear, but could possibly be due to the presence of small *K. brevis* patches or migration of *K. brevis* to depth during the time of satellite observations. The false negatives are also apparent in Fig. 8a, where negative chlorophyll anomalies occur with high counts. Some of these cases were due to the prolonged bloom, especially for the year of 2001.

### 4.2. $b_b$:chlorophyll-a ratio

This approach was successful at separating *K. brevis* blooms from other blooms using *in situ* data, specifically direct chlorophyll-*a* and $b_b$ measurements or chlorophyll-*a* estimates based on *in situ* $R_{rs}$ measurements (Cannizzaro et al., this issue). However, the performance was less satisfactory when chlorophyll-*a* estimates from SeaWiFS were used (Fig. 9).

Fig. 9a shows all data comparisons. By setting a threshold of 0.0013 for $b_b$:chlorophyll-*a* to determine the presence ($>10^3$ counts $L^{-1}$) of *K. Brevis* (i.e., if $b_b$:chlorophyll-*a* is $<0.0013$, *K. Brevis* is present), the probability of success can be as high as 100%. However, it will also miss most of the blooms for which $b_b$:chlorophyll-*a* is $>0.0013$. As suggested by Cannizzaro et al. (this issue), the approach is best applicable in high-chlorophyll-*a* ($>1$–$1.5\,mg\,m^{-3}$) waters. After applying a filter of $1\,mg\,m^{-3}$ for chlorophyll-*a* concentration, the results were improved (Fig. 9b), i.e., lower $b_b$:chlorophyll-*a* ratio generally meant high *K. brevis* counts when chlorophyll-*a* is $>1\,mg\,m^{-3}$. However, applying the chlorophyll-*a* anomaly filter ($>1\,mg\,m^{-3}$, Fig. 9c) does not show significant improvement since too many points were filtered out. In Fig. 9b, a threshold of 0.003 $b_b$:chlorophyll-*a* ratio may be used to indicate presence/absence of *K. brevis* blooms, but not all pixels with $b_b$:chlorophyll-*a* ratio $<0.003$ were associated with high *K. brevis* counts. A close examination of these data points suggested that they come from coastal waters on 3 December 2001. Chlorophyll-*a* concentration and CDOM absorption coefficient at 443 nm ($a_g443$) from the Carder et al. (1999) semi-analytical

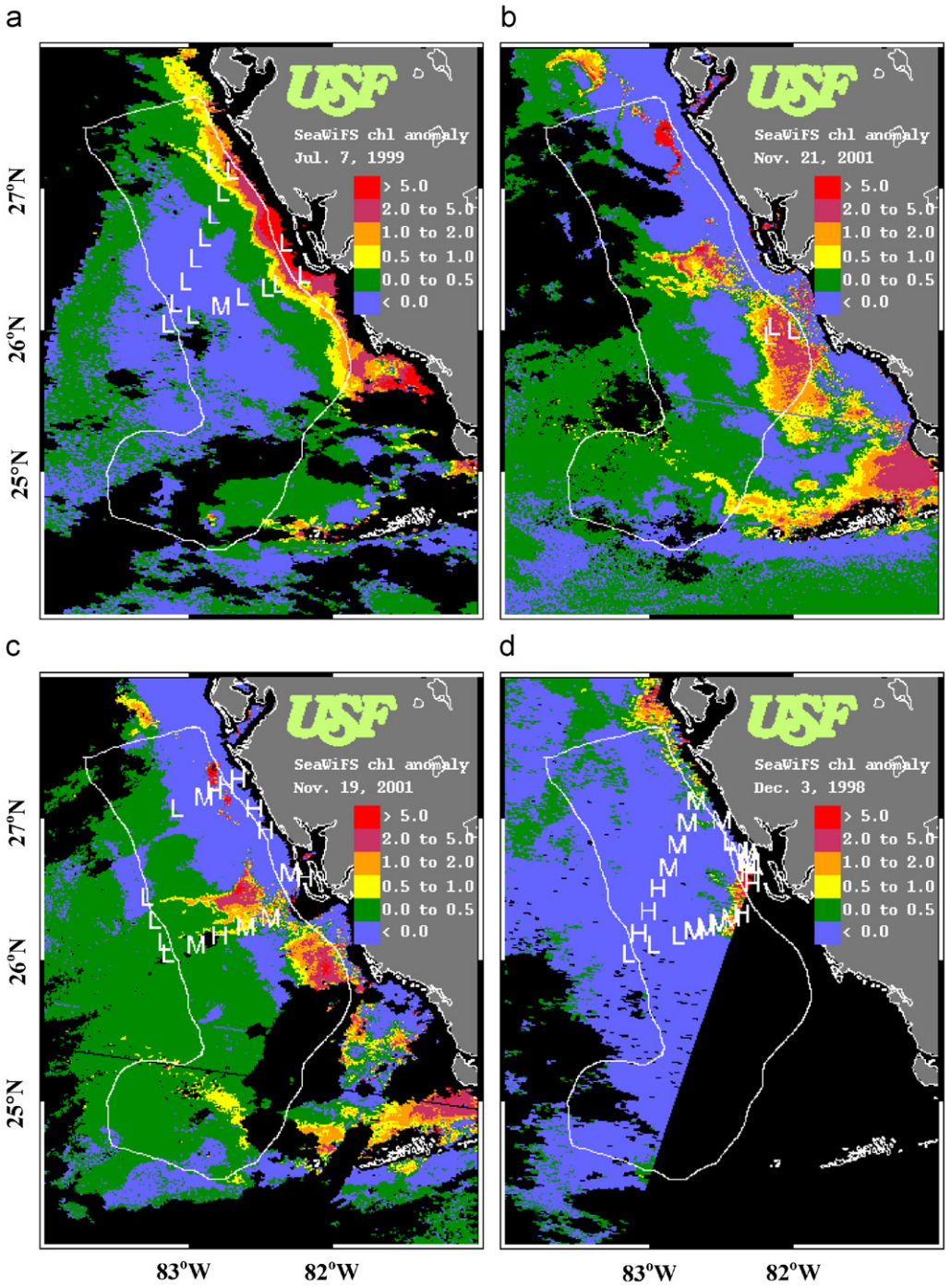


Fig. 7. Chlorophyll–anomaly images from SeaWiFS (OC4 algorithm), showing false positives (a and b) and false negatives (c and d) for *K. brevis* detection. "H," "M," and "L" means high ($>10^5\,L^{-1}$), medium ($<10^5\,L^{-1}$ but $>10^3\,L^{-1}$), and low ($<10^3\,L^{-1}$) *K. brevis* counts, respectively, for the same day.

algorithm were around $1.3\,mg\,m^{-3}$ and $0.13\,m^{-1}$, respectively. At these concentrations, the chlorophyll-*a* absorption coefficient at 443 nm ($a_\phi 443$) is $\sim 0.04 \times 1.3^{0.6} = 0.046\,m^{-1}$ (Bricaud et al., 1995). Therefore, $a_g 443$ was nearly three times of $a_\phi 443$ in these waters. Cannizzaro et al. (this issue) points out

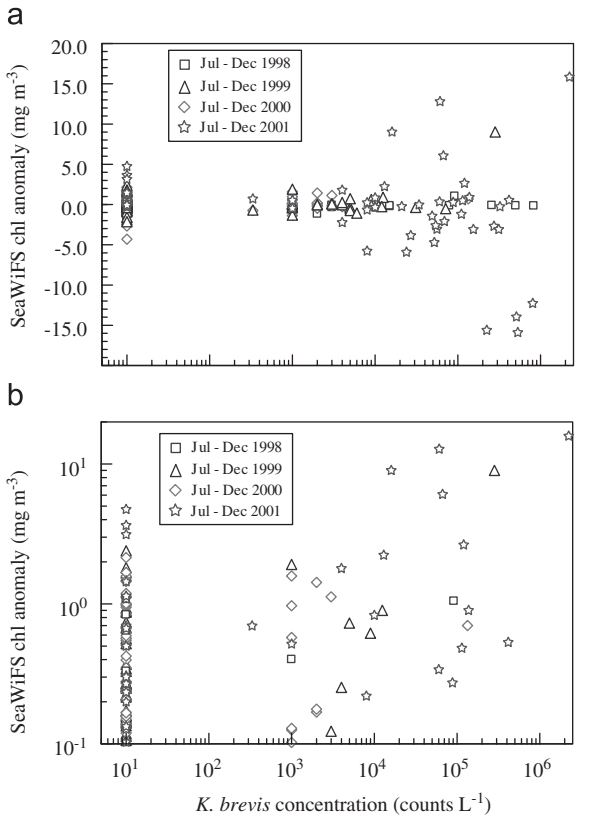


Fig. 8. Comparison of chlorophyll–anomaly (OC4 algorithm) and *K. brevis* concentration from *in situ* sampling between late 1997 and early 2002. Data of 0 counts were artificially changed to 10 in order to display on the log-scaled graph; (a) both positive and negative anomalies are shown and (b) only positive anomalies are shown.

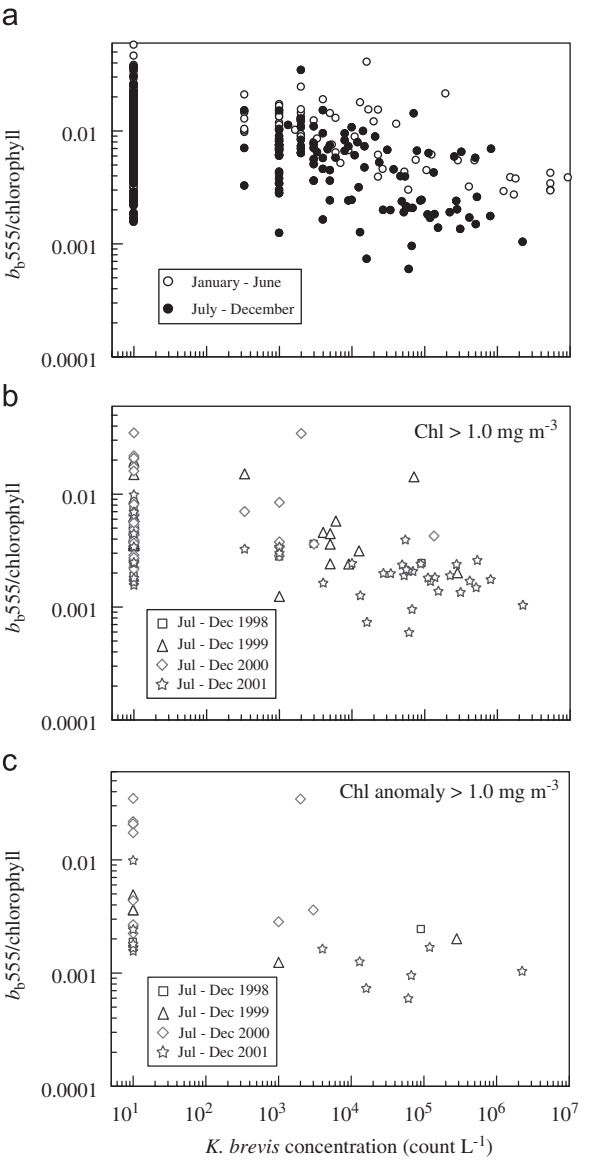


Fig. 9. Comparison of *K. brevis* concentration and ratio between particulate backscattering coefficient at 555 nm ($b_b555$, derived from SeaWiFS with a spectra-matching algorithm; Lee et al., 1999; Hu et al., 2003a) and the SeaWiFS-derived chlorophyll-*a* concentration (OC4 algorithm). (a) All data for the region of interest (outlined in Fig. 3); (b) only summer and fall data with chlorophyll-*a* $>1\,mg\,m^{-3}$ are shown; (c) only summer and fall data with chlorophyll–anomaly $>1\,mg\,m^{-3}$ are shown.

that the $b_b$:chlorophyll-*a* approach is questionable when $a_g443/a_\phi443$ is $>2$. Therefore, $a_g443/a_\phi443$ may be used as a filter to remove the suspicious positives.

Similar to Fig. 6 in Cannizzaro et al. (this issue), Fig. 10 shows $b_b$ versus chlorophyll-*a* for various *K. brevis* concentrations. Clearly, the approach was not applicable for chlorophyll-*a* $<1\,mg\,m^{-3}$, i.e., for these concentrations, high (triangle and diamond) and low (circle and square) *K. brevis* concentrations were indistinguishable. The method was somehow successful in 2001 for chlorophyll-*a* $>1\,mg\,m^{-3}$, while there were still some cases of false positives, i.e., when $b_b$:chlorophyll-*a* was low for chlorophyll-*a* $>1\,mg\,m^{-3}$ (indicating *K. brevis* bloom by the algorithm), actual *K. brevis* concentrations were low (black circles).

Application of the semi-analytical algorithm of Carder et al. (1999) may improve some chlorophyll-*a* estimates in waters with moderate chlorophyll-*a* concentrations (e.g., Hu et al., 2003b). However, use of these chlorophyll-*a* estimates did not lead to significant improvement in *K. brevis* bloom detection, possibly due to imperfect atmospheric correction and uncertainties inherent in the bio-optical algorithm (see below).

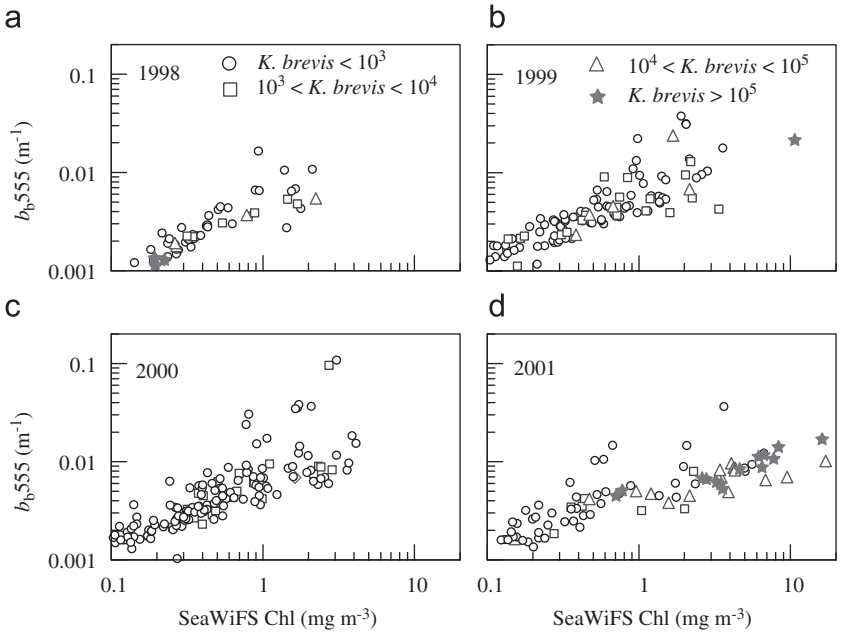


Fig. 10. SeaWiFS-derived chlorophyll concentration (OC4 algorithm) versus particulate backscattering coefficient at 555 nm ($b_b555$) for various *K. brevis* concentration groups. Figure legend applies to all panels.

### 4.3. Spectral analyses

Six case studies (Fig. 11) were chosen to illustrate successes and problems in identifying red tides, namely:

- river plume from the Suwannee runoff (7 June 1998; Jolliff et al., 2003);
- coastal dark water patches of unknown type (7 August 1999);
- *K. brevis* bloom southwest of Charlotte Harbor (17 October 2000; Stumpf et al., 2003a);
- *K. brevis* bloom along the coast (3 October 2001);
- "Black water" near the Florida Keys (4 February 2002; SWFDOG, 2002; Hu et al., 2003a);
- coastal runoff from heavy rainfall (18 October 2003; Hu et al., 2004).

$R_{rs}$ spectra for the high-chlorophyll-*a* anomaly patch in each case are presented in Fig. 11, separated into two groups of different chlorophyll-*a* concentration. Also shown on the figure are the median and standard deviation values of the $R_{rs}$ spectra. The 17 October 2000 *K. brevis* bloom, for example, was a dark feature with low $R_{rs}$ values at all wavelengths, consistent with *in situ* optical observations for typical *K. brevis* blooms (Fig. 2 of Cannizzaro et al., this issue). However, another *K. brevis* bloom on 3 October 2001 showed different $R_{rs}$ spectral shape and magnitude. These were similar to those from a diatom bloom of the "black water" (4 February 2002). $R_{rs}$ spectra from coastal runoff plumes on 7 June 1998 and 18 October 2003 appeared similar to those of the 17 October 2000 *K. brevis* bloom. Clearly, it was difficult to discriminate between various features observed along the coast.

Statistical results based on a standard *t*-mean test (unpaired) of several wavelengths from all six cases in Fig. 11 are shown in Tables 1–3. A test value below 0.05 implies a significant difference between cases. For all wavelengths in the test (412, 443, and 555 nm), most of these river plume, black water, and *K. brevis* events were not significantly different in the $R_{rs}$ spectra. Results for the other three wavelengths (490, 510, and 670 nm) are similar. This helps explain why existing algorithms sometimes fail to differentiate between features. Indeed, if the $R_{rs}$ spectra of two different events are similar, it is impossible to differentiate them optically.

## 5. Discussion

Tomlinson et al. (2004) evaluated the performance of the chlorophyll–anomaly method to identify *K. brevis* blooms in the eastern Gulf of

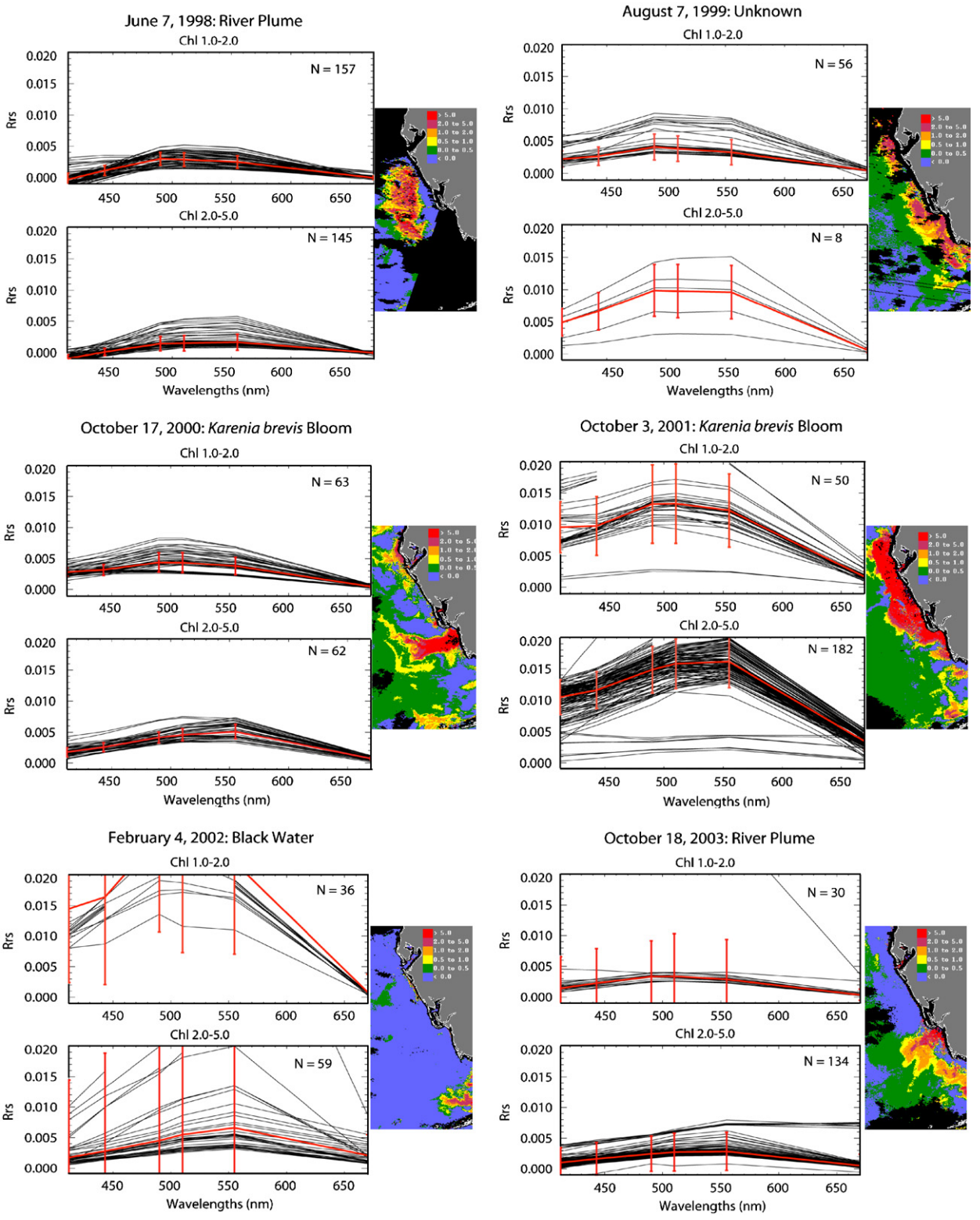


Fig. 11. $R_{rs}$ spectra for various dark water features, obtained from SeaWiFS from the standard NASA processing codes (SeaDAS4.4). Note that the images shows chlorophyll anomaly, while the chlorophyll groups (1–2 and 2–5) use absolute concentrations.

Table 1
*t*-Mean test results between average $R_{rs}$ values at 412 nm for the six cases shown in Fig. 11

| | 6/7 River | 10/17 Kbreve | 10/3 Kbreve | 2/4 Blackwater | 10/18 River | 8/7 Unknown |
|---|---|---|---|---|---|---|
| *Low CHL (2–5 mg m$^{-3}$)* | | | | | | |
| 6/7 River | −999 | −999 | −999 | −999 | −999 | −999 |
| 10/17 Kbreve | −999 | 1.00 | 0.12 | **<0.01** | 0.17 | **<0.01** |
| 10/3 Kbreve | −999 | 0.12 | 1.00 | **<0.01** | 0.46 | 0.42 |
| 2/4 Blackwater | −999 | **<0.01** | **<0.01** | 1.00 | 0.08 | 0.07 |
| 10/18 River | −999 | 0.17 | 0.46 | 0.08 | 1.00 | **0.01** |
| 8/7 Unknown | −999 | **<0.01** | 0.42 | 0.07 | **0.01** | 1.00 |
| *Mid CHL (2–5 mg m$^{-3}$)* | | | | | | |
| 6/7 River | 1.00 | 0.78 | 0.18 | **<0.01** | 0.67 | 0.25 |
| 10/17 Kbreve | 0.78 | 1.00 | 0.10 | **<0.01** | 0.76 | **0.01** |
| 10/3 Kbreve | 0.18 | 0.10 | 1.00 | **0.01** | 0.22 | 0.31 |
| 2/4 Blackwater | **0.00** | **<0.01** | **0.01** | 1.00 | **<0.01** | 0.96 |
| 10/18 River | 0.67 | 0.76 | 0.22 | **<0.01** | 1.00 | 0.09 |
| 8/7 Unknown | 0.25 | **0.01** | 0.31 | 0.96 | 0.09 | 1.00 |

Values below 0.05 (those bolded) mean that the $R_{rs}$ between the two cases is significantly different.

Table 2
Same as Table 1 but the wavelength is 443 nm

| | 6/7 River | 10/17 Kbreve | 10/3 Kbreve | 2/4 Blackwater | 10/18 River | 8/7 Unknown |
|---|---|---|---|---|---|---|
| *Low CHL (1–2 mg m$^{-3}$)* | | | | | | |
| 6/7 River | −999 | −999 | −999 | −999 | −999 | −999 |
| 10/17 Kbreve | −999 | 1.00 | 0.15 | **<0.01** | 0.20 | **<0.01** |
| 10/3 Kbreve | −999 | 0.15 | 1.00 | **0.02** | 0.42 | 0.32 |
| 2/4 Blackwater | −999 | **<0.01** | **0.02** | 1.00 | 0.08 | 0.21 |
| 10/18 River | −999 | 0.20 | 0.42 | 0.08 | 1.00 | **0.01** |
| 8/7 Unknown | −999 | **<0.01** | 0.32 | 0.21 | **0.01** | 1.00 |
| *Mid CHL (2–5 mg m$^{-3}$)* | | | | | | |
| 6/7 River | 1.00 | 0.53 | 0.44 | 0.30 | 0.88 | 0.21 |
| 10/17 Kbreve | 0.53 | 1.00 | 0.07 | 0.05 | 0.21 | **<0.01** |
| 10/3 Kbreve | 0.44 | 0.07 | 1.00 | 0.49 | 0.40 | 0.23 |
| 2/4 Blackwater | 0.30 | 0.05 | 0.49 | 1.00 | 0.20 | 0.61 |
| 10/18 River | 0.88 | 0.21 | 0.40 | 0.20 | 1.00 | **0.04** |
| 8/7 Unknown | 0.21 | **<0.01** | 0.23 | 0.61 | **0.04** | 1.00 |

Mexico. They concluded that the method accurately identified *K. brevis* blooms >83% of the time. However, they only considered the "bloom season" from 1 August to 30 April, and most of the events were confirmed non-bloom cases. In reality, red tides occur at any time of the year and may last for more than a year, for example from December 2004 to January 2006 (Hu et al., 2006). Using the same datasets but making comparisons using satellite and *in situ* matching data pairs, the skill of the assessments is lower (Fig. 5). Certainly, many points may not be independent in Fig. 5, with multiple points representing a single event. However, in the perspective of red tide monitoring, we need to not only detect (ideally, predict) events, but also assess the red tide spatial distribution and temporal duration. The NOAA chlorophyll–anomaly method effectively detects "new" blooms, but it is most effective identifying non-bloom waters. Some of the false positives may have been due to the coarse resolution of satellite sensors (~1 km$^2$ pixel$^{-1}$), which helps detect red tides even when field samples miss *K. brevis* patches and vice versa. This suggests that future satellite sensors should have better spatial resolution for coastal monitoring of red tide patches. Ideally, they should also have more spectral bands to correct for bottom effects.

Table 3
Same as Table 1 but the wavelength is 555 nm

| | 6/7 River | 10/17 Kbreve | 10/3 Kbreve | 2/4 Blackwater | 10/18 River | 8/7 Unknown |
|---|---|---|---|---|---|---|
| *Low CHL (1–2 mg m$^{-3}$)* | | | | | | |
| 6/7 River | −999 | −999 | −999 | −999 | −999 | −999 |
| 10/17 Kbreve | −999 | 1.00 | 0.87 | **<0.01** | **<0.01** | **<0.01** |
| 10/3 Kbreve | −999 | 0.87 | 1.00 | **<0.01** | 0.19 | 0.22 |
| 2/4 Blackwater | −999 | **<0.01** | **<0.01** | 1.00 | 0.53 | **<0.01** |
| 10/18 River | −999 | **<0.01** | 0.19 | 0.53 | 1.00 | **<0.01** |
| 8/7 Unknown | −999 | **<0.01** | 0.22 | **<0.01** | **<0.01** | 1.00 |
| *Mid CHL (2–5 mg m$^{-3}$)* | | | | | | |
| 6/7 River | 1.00 | 0.87 | 0.20 | 0.05 | 0.26 | 0.09 |
| 10/17 Kbreve | 0.87 | 1.00 | 0.15 | **0.03** | 0.20 | 0.28 |
| 10/3 Kbreve | 0.20 | 0.15 | 1.00 | 0.05 | 0.73 | 0.22 |
| 2/4 Blackwater | 0.05 | **0.03** | 0.05 | 1.00 | 0.13 | 0.51 |
| 10/18 River | 0.26 | 0.20 | 0.73 | 0.13 | 1.00 | 0.41 |
| 8/7 Unknown | 0.09 | 0.28 | 0.22 | 0.51 | 0.41 | 1.00 |

The challenge remains in identifying a phytoplankton bloom as being *K. brevis* or other phytoplankton. The $b_b$:chlorophyll-*a* ratio is effective in this regard when applied using *in situ* bio-optical optical data (Cannizzaro et al., this issue), but not with satellite ocean color data from SeaWiFS. The difficulty may result from the compounding of problems introduced by low-chlorophyll-*a* patches containing *K. brevis*, patches dominated by CDOM, and shallow waters, as suggested by Cannizzaro et al. (this issue).

CDOM delivered to the ocean by coastal runoff or as a product of decomposition of phytoplankton blooms is often misinterpreted as chlorophyll by band-ratio algorithms. Our subregion of study within the west Florida shelf was carefully outlined to yield matched-up field and satellite observations while partially avoiding river plumes and shallow bottom. However, some coastal inputs are inevitable, especially in the vicinity of Charlotte Harbor. In these cases there are large uncertainties associated with bio-optical and atmospheric correction algorithms (e.g., Hu et al., 2005).

In principle, inherent optical properties (IOPs of the water, e.g., $a$ and $b_b$) may be derived from $R_{rs}(\lambda)$ with bio-optical inversion algorithms (e.g., Carder et al., 1999; Lee et al., 1999; Lee et al., 2002; Maritorena et al., 2002). The concentration of various optical constituents (e.g., chlorophyll-*a*, CDOM) is often estimated using empirical regressions (e.g., Gordon et al., 1983; O'Reilly et al., 2000; Kahru and Mitchell, 2001), due to insufficient knowledge of IOPs. These algorithms have inherent uncertainties derived from scatter in the input datasets. Of particular concern is the fundamental difficulty of estimating chlorophyll-*a* concentrations in CDOM-rich waters. Small concentrations of CDOM lead to large errors in chlorophyll-*a* estimates. The Carder et al. semi-analytical algorithm, implemented in SeaDAS, helps improve chlorophyll-*a* estimates in moderately colored waters (Hu et al., 2003c). However, in very dark waters (high CDOM concentration), this algorithm switches to a band-ratio, again resulting in large uncertainties in chlorophyll estimates. An alternative approach has been proposed by Maritorena et al. (2002) to estimate CDOM and chlorophyll-*a* simultaneously. This method yields chlorophyll-*a* estimates similar to the OC4 algorithm chlorophyll, which suggests that it suffers from the same problems in turbid coastal waters.

Hence, a basic priority for synoptic remote sensing of red tides is to improve the bio-optical algorithms used to estimate chlorophyll-*a* concentrations in shallow or turbid waters. Further, atmospheric correction schemes need to improve to provide better retrievals of $R_{rs}(\lambda)$ over dark coastal waters. For example, we currently obtained incorrect, negative $R_{rs}$ values within highly turbid waters in several images, for example in the 7 June 1998 image of a river plume (Fig. 11) and in the extensive October 2001 *K. brevis* blooms. Improvements in atmospheric correction will also improve results obtained with the NOAA chlorophyll–anomaly approach, which at present may contain large uncertainties.

Sediment resuspension events can be easily identified and differentiated as non-red tide events. This may be accomplished using a predefined $R_{rs}$ threshold (Wynne et al., 2005) or visual examination of RGB composite imagery (Hu et al., 2005). These events frequently appear as bright features in an image.

Once a dark feature is identified, it is useful to examine MODIS fluorescence line height imagery since this can be an effective tool to differentiate between blooms and CDOM-rich river plumes (Hu et al., 2005). Other ancillary information such as wind, ocean currents, and SST imagery from either the Advanced Very High Resolution Radiometer (AVHRR) or MODIS helps understand the environmental context and constrain bloom trajectory forecasts generated by numerical or other models. Such predictions can be verified by time series' of satellite images. Increasing the number of satellite visits per day is therefore a need to enable synoptic coastal water quality assessments. While a combination of SeaWiFS and the two MODIS sensors provides a minimal dataset to accomplish this, new concepts including geostationary ocean color satellite sensors should be considered in designing the next generation of environmental observation satellites.

## 6. Summary and conclusion

*K. brevis* blooms, diatom blooms, and coastal runoff plumes all appear dark on satellite imagery because both phytoplankton and dissolved matter contained in them strongly absorb blue and blue-green light. While differentiating blooms from plumes and other shallow water features (bottom, sediment) is possible using a combination of different types of satellite imagery, discriminating between various types of blooms is more difficult.

Two approaches were tested for *K. brevis* bloom detection. The first one was based on the NOAA chlorophyll–anomaly technique (Stumpf et al., 2003a). Comparison with ~5 years of *K. brevis* data from field surveys and daily chlorophyll–anomaly imagery suggested that the method was successful in some instances in identifying *K. brevis* bloom patches, but that it also yielded false positives and false negatives. An anomaly patch typically greater than 1000 $km^2$ between the 10- and 50-m isobaths was identified in most daily imagery collected in late summer and fall over the entire 1997–2002 series, even during periods when no red tides were reported. Use of ancillary information and historical imagery may improve the success rate of this operational method.

The $b_b$:chlorophyll-*a* ratio method was originally developed and validated with *in situ* data (Cannizzaro et al., this issue). This approach did not yield satisfactory results using SeaWiFS data, possibly due to the uncertainties in the SeaWiFS-derived chlorophyll-*a* and backscattering ($b_b$) products. Examination of the $R_{rs}$ spectra along the coast derived from SeaWiFS images shows that different features can have nearly identical spectra. This complicates automated discrimination of *K. brevis* blooms in an operational setting.

These techniques are not designed to be applied "blindly." For example, NOAA's CoastWatch program uses the chlorophyll–anomaly estimates combined with historical knowledge and ancillary information to determine if a red tide warning should be issued. At present, use of a combination of chlorophyll-*a* concentration, chlorophyll–anomaly, $R_{rs}$ RGB composite, backscattering:chlorophyll-*a* ratio, and MODIS fluorescence data can significantly improve data interpretation in terms of differentiating blooms, plumes, sediment, and shallow bottom.

*In situ* optical data can be used to differentiate *K. brevis* blooms from other blooms. This suggests that the performance of operational and research assessments by remote sensing can be improved by designing better bio-optical and atmospheric correction algorithms. These should be viewed as priorities in coastal operational work focused on water quality monitoring and resource management in the ongoing effort to establish regional coastal ocean observation systems.

## Acknowledgments

This work was supported by the National Aeronautics and Space Administration (NASA) and by the Florida Department of Environmental Protection (FDEP). *K. brevis* counts data were collected by the EcoHAB and HyCODE program participants as well as by volunteers. The data were assembled and provided by the Florida Fish and Wildlife Research Institute (FWRI). We thank Dr. Gabriel Vargo and Merrie Beth Neely (USF) for their guidance and assistance during the cruise series and data analysis. We are also indebted to two anonymous reviewers whose critical comments helped improved this manuscript. SeaWiFS data are

property of Orbimage Corp., and their use here is in accordance with the SeaWiFS Research Data Use Terms and Conditions Agreement of the NASA SeaWiFS project. IMaRS contribution 19.

## Reference

Anderson, D.M., 1995. ECOHAB: The Ecology and Oceanography of Harmful Algal Blooms, a National Research Agenda. Woods Hole Oceanographic Institute, Woods Hole, MA, 67pp.

Arnone, R.A., Martinolich, P., Gould Jr., R.W., Stumpf, R., Ladner, S., 1998. Coastal optical properties using SeaWiFS. In: Ocean Optics XIV, Kailua Kona, Hawaii, USA.

Bailey, S.W., McCLain, C.R., Werdell, P.J., Schieber, B.D., 2000. Normalized water-leaving radiance and chlorophyll *a* match-up analyses In: Hooker, S.B., Firestone, E.R. (Eds.), SeaWiFS Postlaunch Technical Report Series, NASA Technical Memorandum 2000-206892, vol. 10, pp. 45–52 (Chapter 7).

Balch, W.M., Holligan, P.M., Ackleson, S.G., Voss, K.J., 1991. Biological and optical properties of mesoscale coccolithophore blooms in the Gulf of Maine. Limnology and Oceanography 36, 629–643.

Brand, L., Compton, A., 2007. Long-term increase in *Karenia brevis* abundance along the Southwest Florida Coast. Harmful Algae 6 (2), 232–252.

Bricaud, A., Babin, M., Morel, A., Claustre, H., 1995. Variability in the chlorophyll-specific absorption coefficients of natural phytoplankton: analysis and parameterization. Journal of Geophysical Research 100, 13,321–13,332.

Cannizzaro, J.P., Carder, K.L., Chen, F.R., Heil, C.A., Vargo, G.A., this issue. A novel technique for detection of the toxic dinoflagellate *Karenia brevis* in the Gulf of Mexico from remotely sensed ocean color data. Continental Shelf Research.

Carder, K.L., Chen, F.R., Lee, Z.P., Hawes, S.K., KamyKowski, D., 1999. Semianalytic moderate-resolution imaging spectrometer algorithms for chlorophyll *a* and absorption with bio-optical domains based on nitrate depletion temperatures. Journal of Geophysical Research 104, 5403–5421.

Cullen, J.J., Ciotti, A.M., Davis, R.F., Lewis, M.R., 1997. Optical detection and assessment of algal blooms. Limnology and Oceanography 42, 1223–1239.

Esaias, E., Abbott, M., Barton, I., et al., 1998. An overview of MODIS capabilities for ocean science observations. IEEE Transactions on Geoscienc and Remote Sensing 36, 1250–1265.

Evens, T.J., Kirkpatrick, G.J., Millie, D.F., Chapman, D.J., Schofield, O.M.E., 2001. Photophysiological responses of the toxic red-tide dinoflagellate *Gymnodinium breve* (Dinophyceae) under natural sunlight. Journal of Plankton Research 23, 1177–1193.

Gordon, H.R., Wang, M., 1994. Retrieval of water-leaving radiance and aerosol optical thickness over the oceans with SeaWiFS: a preliminary algorithm. Applied Optics 33, 443–452.

Gordon, H.R., Clark, D.K., Brown, J.W., Brown, O.B., Evans, R.H., Broenkow, W.W., 1983. Phytoplankton pigment concentrations in the middle Atlantic bight: comparison between ship determination and Coastal Zone Color Scanner estimates. Applied Optics 22, 20–36.

Hu, C., Carder, K.L., Muller-Karger, F.E., 2001. How precise are SeaWiFS ocean color estimates? Implications of digitization-noise errors. Remote Sensing of Environment 76, 239–249.

Hu, C., Hackett, K.E., Callahan, M.K., Andréfouët, S., Wheaton, J.L., Porter, J.W., Muller-Karger, F.E., 2003a. The 2002 ocean color anomaly in the Florida Bight: a cause of local coral reef decline? Geophysical Research Letters 30 (3), 1151.

Hu, C., Lee, Z.P., Muller-Karger, F.E., Carder, K.L., 2003b. Application of an optimization algorithm to satellite ocean color imagery: a case study in Southwest Florida coastal waters. In: Frouin, R.J., Yuan, Y., Kawamura, H. (Eds.), Ocean Remote Sensing and Applications: 24–26 October, 2002, Hangzhou, China (Proceedings of Spie—The International Society for Optical Engineering). SPIE, Bellingham, WA, pp. 70–79.

Hu, C., Muller-Karger, F.E., Biggs, D.C., Carder, K.L., Nababan, B., Nadeau, D., Vanderbloemen, J., 2003c. Comparison of ship and satellite bio-optical measurements on the continental margin of the NE Gulf of Mexico. International Journal of Remote Sensing 24, 2597–2612.

Hu, C., Muller-Karger, F.E., Vargo, G.A., Neely, M.B., 2004. Linkages between coastal runoff and the Florida Keys ecosystem: a study of a dark plume event. Geophysical Research Letters 31, L15307.

Hu, C., Muller-Karger, F.E., Taylor, C., Carder, K.L., Kelble, C., Johns, E., Heil, C.A., 2005. Red tide detection and tracing using MODIS fluorescence data: a regional example in SW Florida coastal waters. Remote Sensing of Environment 97, 311–321.

Hu, C., Muller-Karger, F.E., Swarzenski, P.W., 2006. Hurricanes, submarine groundwater discharge, and Florida's red tides. Geophysical Research Letters 33, L11601.

Jolliff, J.K., Walsh, J.J., He, R., Weisberg, R.H., Stovall-Leonard, A., Coble, P.G., Comny, R., Heil, C., Nababan, B., Zhang, H., Hu, C., Muller-Karger, F.E., 2003. Dispersal of the Suwannee River plume over the West Florida shelf. Simulation and observation of the optical and biochemical consequences of a flushing event. Geophysical Research Letters 30 (13).

Kahru, M., Mitchell, B.G., 2001. Seasonal and non-seasonal variability of satellite-derived chlorophyll and CDOM concentration in the California Current. Journal of Geophysical Research 106 (C2), 2517–2529.

Kirkpatrick, G.J., Millie, D.F., Moline, M.A., Schofield, O., 2000. Optical discrimination of a phytoplankton species in natural mixed populations. Limnology and Oceanography 45 (2), 467–471.

Lee, Z., Carder, K.L., Mobley, C.D., Steward, R.G., Patch, J.S., 1999. Hyperspectral remote sensing for shallow waters: 2. Deriving bottom depths and water properties by optimization. Applied Optics 38, 3831–3843.

Lee, Z., Carder, K.L., Arnone, R.A., 2002. Deriving inherent optical properties from water color: a multiband quasi-analytical algorithm for optically deep waters. Applied Optics 41, 5755–5772.

Lohrenz, S.E., Fahnenstiel, G.L., Kirkpatrick, G.J., Carroll, C.L., Kelly, K.A., 1999. Microphotometric assessment of spectral absorption and its potential application for

characterization of harmful algal species. Journal of Phycology 35, 1438–1446.

Maritorena, S., Siegel, D.A., Peterson, A.R., 2002. Optimization of a semianalytical ocean color model for global-scale applications. Applied Optics 41, 2705–2714.

McClain, C.R., Cleave, M.L., Feldman, G.C., Gregg, W.W., Hooker, S.B., Kuring, N., 1998. Science quality SeaWiFS data for global biosphere research. Sea Technology 39, 10–16.

Millie, D.F., Schofield, O., Kirkpatrick, G.J., Johnsen, G., Tester, P.A., Vinyard, B.T., 1997. Phytoplankton pigments and absorption spectra as potential 'Biomarkers' for harmful algal blooms: a case study of the Florida red-tide dinoflagellate, *Gymnodinium breve*. Limnology and Oceanography 42, 1240–1251.

Morton, R.A. and Burklew, M.A., 1969. Florida shellfish toxicity following blooms of dinoflagellate *Gymnodium breve*. Florida Department of Natural Resources Marine Laboratory, Technical Series No. 60, 26pp.

O'Reilly, J.E., et al., 2000. Ocean color chlorophyll a algorithms for SeaWiFS, OC2, and OC4: version 4. In: Hooker, S.B. & Firestone, E.R. (Eds.), SeaWiFS Postlaunch Technical Report Series, NASA Technical Memorandum 2000-206892, vol. 11, 51pp.

Schofield, O., Grzymski, J., Bissett, W.P., Kirkpatrick, G.J., Millie, D.F., Moline, M., Roesler, C.S., 1999. Optical monitoring and forecasting systems for harmful algal blooms: possibility or pipe dream? Journal of Phycology 35, 1477–1496.

Steidinger, K.A., Ingle, R.M., 1972. Observations on the 1971 summer red tide in Tampa Bay. Florida Environmental Letters 3 (4), 271–277.

Steidinger, K.A., Joyce, E.A., 1973. Florida red tide. Florida Department of Natural Rescources Report No. 17, 26pp.

Steidinger, K.A., Haddad, K., 1981. Biologic and hydrographic aspects of red tides. Bioscience 31 (11), 814–819.

Steidinger, K.A., Vargo, G.A., Tester, P.A., Tomas, C.R., 1998. Bloom dynamics and physiology of *Gymnodinium breve*, with emphasis on the Gulf of Mexico. In: Anderson, E.M., Cembella, A.D., Hallengraff, G.M. (Eds.), Physiological Ecology of Harmful Algal Blooms. Springer, New York, pp. 135–153.

Stumpf, R.P., 2001. Applications of satellite ocean color sensors for monitoring and predicting Harmful Algal Blooms. Human and Ecological Risk Assessment 7, 1363–1368.

Stumpf, R.P., Culver, M.E., Tester, P.A., Tomlinson, M., Kirkpatrick, G.J., Pederson, B.A., Truby, E., Ransibrahmanakul, V., Soracco, M., 2003a. Monitoring *Karenia brevis* blooms in the Gulf of Mexico using satellite ocean color imagery and other data. Harmful Algae 35, 1–14.

Stumpf, R.P., Arnone, R.A., Gould Jr., R.W., Martinolich, P.M., Ransibrahmanakul, V., 2003b. A partially coupled ocean–
atmosphere model for retrieval of water-leaving radiance from SeaWiFS in coastal waters. In: Hooker, S.B., Firestone, E.R. (Eds.), SeaWiFS Postlaunch Technical Report Series, NASA Technical Memorandum, 2003-206892, vol. 22, 74pp.

Subramaniam, A., Carpenter, E.J., Falkowski, P.G., 1999. Bio-optical properties of the marine diazotrophic cyanobacteria *Trichodesmium* spp. II. A reflectance model for remote sensing. Limnology and Oceanography 44, 618–627.

SWFDOG, 2002. Satellite images track ''black water'' event off Florida coast. EOS Transcript AGU 83, 281–285.

Tester, P.A., Steidinger, K.A., 1997. *Gymnodinium breve* red tide blooms: initiation, transport, and consequences of surface circulation. Limnology and Oceanography 42, 1039–1051.

Tomlinson, M.C., Stumpf, R.P., Ransibrahmanakul, V., Truby, E.W., Kirkpatrick, G.J., Pederson, B.A., Vargo, G.A., Heil, C.A., 2004. Evaluation of the use of SeaWiFS imagery for detection *Karenia brevis* blooms in the eastern Gulf of Mexico. Remote Sensing of Environment 91, 293–303.

Walsh, J.J., Steidinger, K.A., 2001. Saharan dust and Florida red tides: the cyanophyte connection. Journal of Geophysical Research 106, 11,597–11,612.

Walsh, J.J., Jolliff, J.K., Darrow, B.P., Lenes, J.M., Milroy, S.P., Remsen, A., Dieterle, D.A., Carder, K.L., Chen, F.R., Vargo, G.A., Weisberg, R.H., Fanning, K.A., Muller-Karger, F.E., Shinn, E., Steidinger, K.A., Heil, C.A., Tomas, C.R., Prospero, J.S., Lee, T.N., Kirkpatrick, G.J., Whitledge, T.E., Stockwell, D.A., Villareal, T.A., Jochens, A.E., Bontempi, P.S., 2006. Red tides in the Gulf of Mexico: where, when, and why? Journal of Geophysical Research 111, C11003.

Williams, J., Ingle, R.M., 1972. Ecological note on Gonyaulax momlata (Dinophyceae). Florida Department of Natural Resources Marine Laboratory Leaf Series, vol 1, Part 1, No. 5, 12pp.

Wynne, T.T., Stumpf, R.P., Tomlinson, M.C., Ransibrahmanakul, V., Villareal, T.A., 2005. Detecting *Karenia brevis* blooms and algal resuspension in the western Gulf of Mexico with satellite ocean color imagery. Harmful Algae 4, 992–1003.

Zhang, H., 2002. Detecting red tides on the West Florida Shelf by classification of SeaWiFS satellite imagery. Master's Thesis, Department of Computer Science and Engineering, University of South Florida.

Zhang, M., Hall, L.O., Muller-Karger, F.E., Goldgof, D.B., 2000. Knowledge-guided classification of coastal zone color images off the West Florida Shelf. International Journal of Pattern Recognition and Artificial Intelligence 14 (8), 987–1007.